Electronic Supplementary Material (ESI) for Physical Chemistry Chemical Physics.
This journal is © The Royal Society of Chemistry 2023

Supporting Information

# Elucidating TH301's Influence on the Torsion Angle of CRY1 W399 Using Replica Exchange with Solute Tempering (REST) Molecular Dynamics (MD) Simulations

Yeongrae Cho,‡[a,c], Kexin Li,‡ [a, c], Jin Hyup Lee [b,c], Seung Pil Pack[a,c] and Art E. Cho*[a,c]

a. *Department of Bioinformatics, Korea University, 2511 Sejong-ro, Sejong, 30119, Korea*
b. *Department of Food and Biotechnology, 2511 Sejong-ro, Sejong, 30119, Korea*
c. *Biological Clock-based Anti-aging Convergence RLRC, Korea University, Sejong, Republic of Korea*

*Correspondence: artcho@korea.ac.kr

‡These authors contributed equally to this work

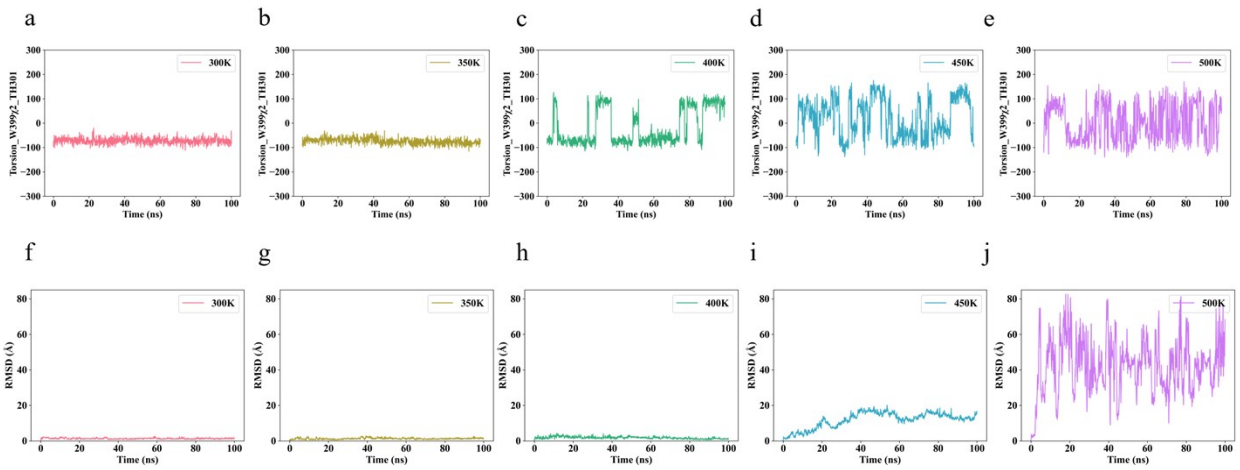


**S-Fig 1.** MD simulations of the CRY1-TH301 complex spanned temperatures from 300K to 500K, incrementing at 50K intervals, over a duration of 100ns. We evaluated the torsion angle χ2 of W399 (a-e) and the RMSD of the ligand (f-j). Specifically, (a & f) correspond to 300K, (b & g) to 350K, (c & h) to 400K, (d & i) to 450K, and (e & j) to 500K.

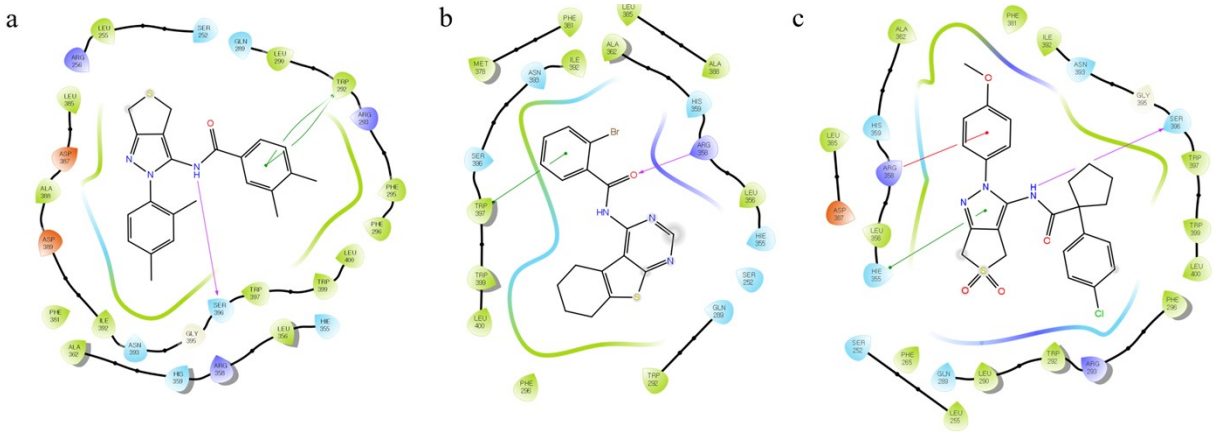


**S-Fig 2**. 2D diagram representations of the docking simulation results for each ligand at the binding site of the target protein CRY, with residues within 5Å displayed. (a) Interaction between KL101 and CRY1, (b) Interaction between KL201 and CRY1 and (c) Interaction between TH301 and CRY1.

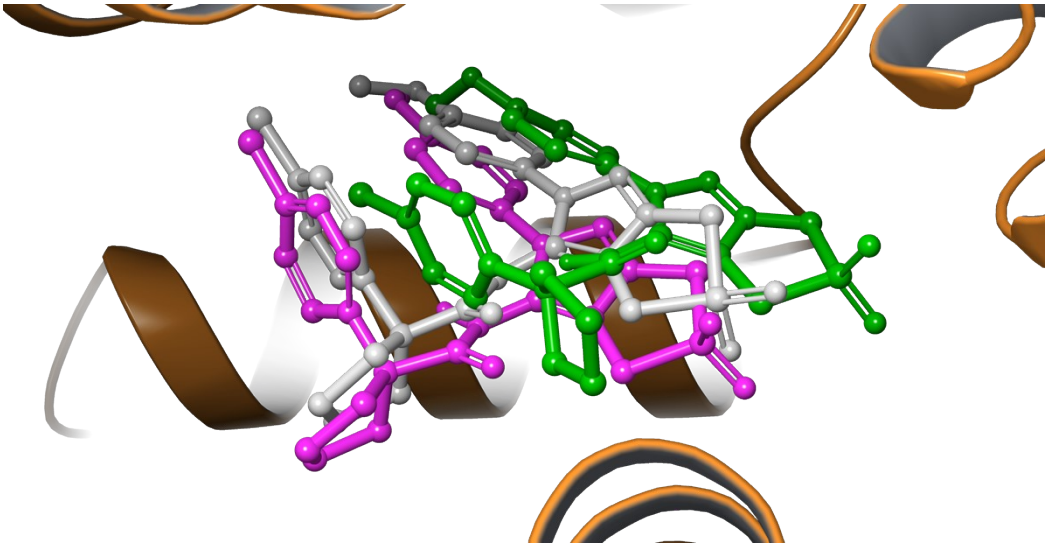

**S-Fig 3.** Comparison and alignment of the binding pose between the crystal structure (PDB: 6KX7) and simulation results. Representations include the crystal structure (white), the initial structure from the MD simulation and docking result (green), and the average structure derived from the MD simulation (magenta).

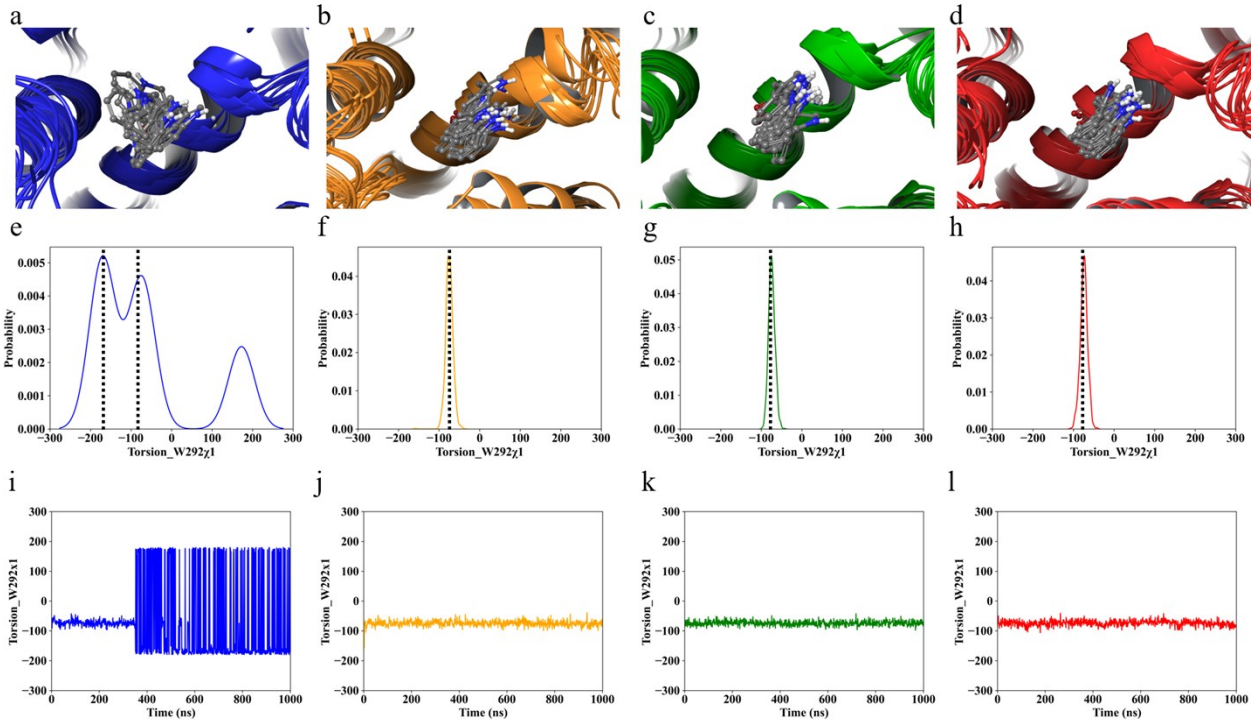


**S-Fig 4.** The torsion angle of CRY1's W292 during the MD simulation is illustrated. This is achieved by extracting 10 snapshots at intervals of every 100 ns (a-d). The KDE plot shows the distribution of CRY1's W292 χ1(e-h) torsion angle across all simulation frames, with dashed lines denoting angles discerned in the CRY1 crystal structure. Linear graphs (i-l) present the progression of the torsion angle of W292 over time. The colors represent different structures: Apo (Blue), TH301 (Yellow), KL101 (Green), and KL201 (Red).

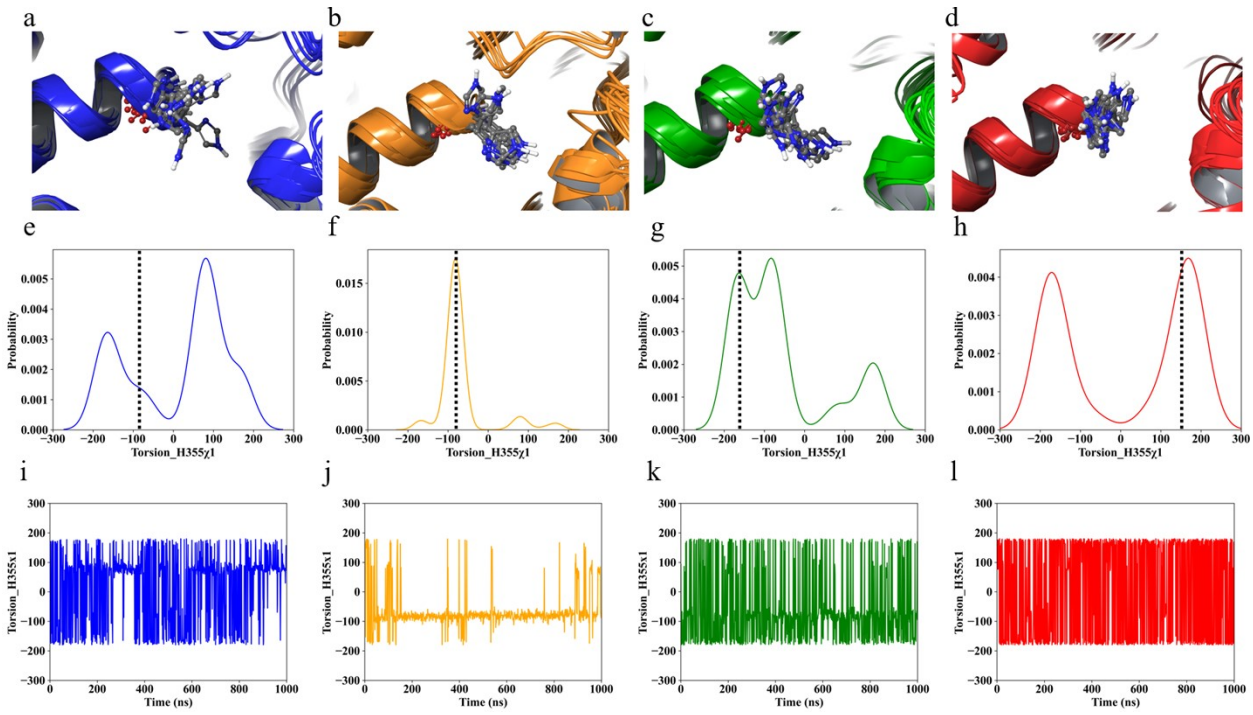


**S-Fig 5.** The torsion angle of CRY1's H355 during the MD simulation is illustrated. This is achieved by extracting 10 snapshots at intervals of every 100 ns (a-d). The KDE plot shows the distribution of CRY1's H355 χ1(e-h) torsion angle across all simulation frames, with dashed lines denoting angles discerned in the CRY1 crystal structure. Linear graphs (i-l) present the progression of the torsion angle of H355 over time. The colors represent different structures: Apo (Blue), TH301 (Yellow), KL101 (Green), and KL201 (Red).

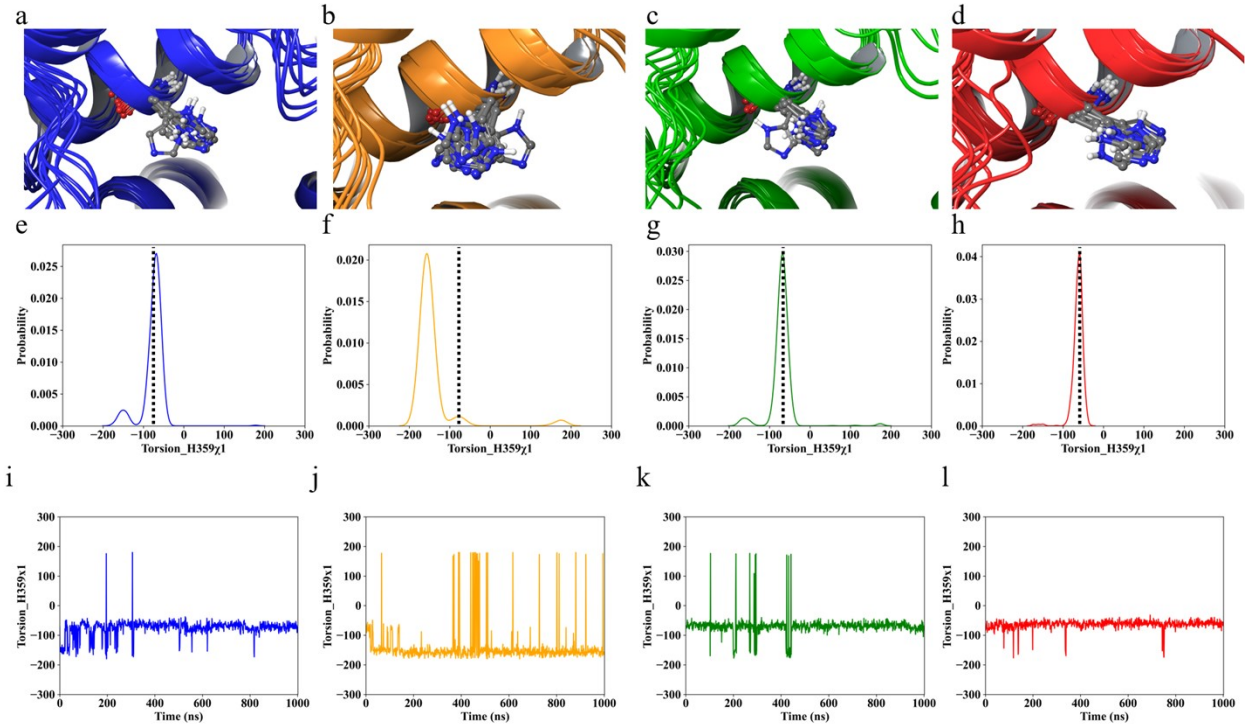


**S-Fig 6.** The torsion angle of CRY1's H359 during the MD simulation is illustrated. This is achieved by extracting 10 snapshots at intervals of every 100 ns (a-d). The KDE plot shows the distribution of CRY1's H359 χ1 (e-h) torsion angle across all simulation frames, with dashed lines denoting angles discerned in the CRY1 crystal structure. Linear graphs (i-l) present the progression of the torsion angle of H359 over time. The colors represent different structures: Apo (Blue), TH301 (Yellow), KL101 (Green), and KL201 (Red).

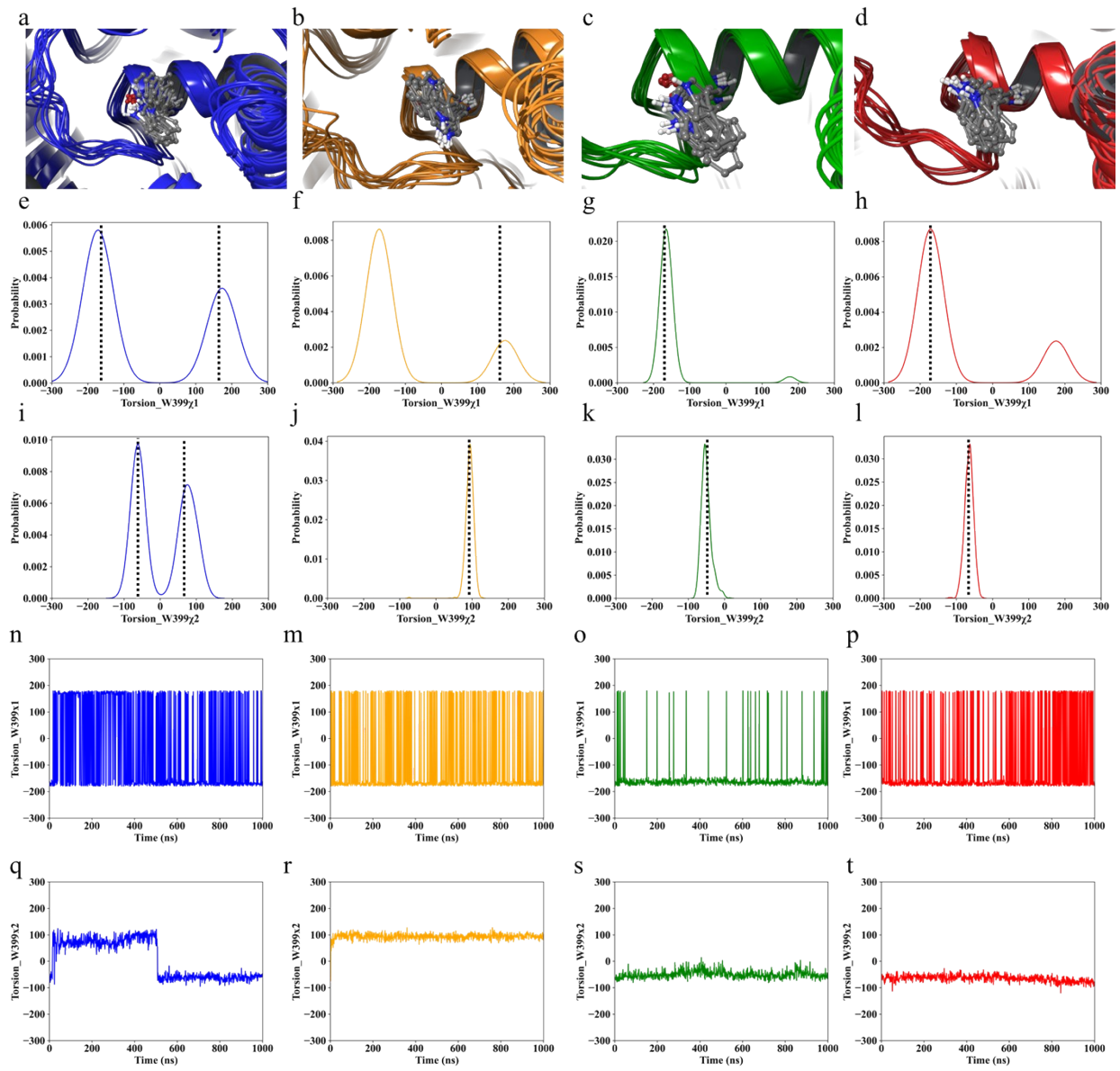


**S-Fig 7.** The torsion angle of CRY1's W399 during the MD simulation is illustrated. This is achieved by extracting 10 snapshots at intervals of every 100 ns (a-d). The KDE plot shows the distribution of CRY1's W399 χ1 (e-h) and χ2 (i-l) torsion angle across all simulation frames, with dashed lines denoting angles discerned in the CRY1 crystal structure. Linear graphs (n-t) present the progression of the torsion angle of W399 over time. The colors represent different structures: Apo (Blue), TH301 (Yellow), KL101 (Green), and KL201 (Red).

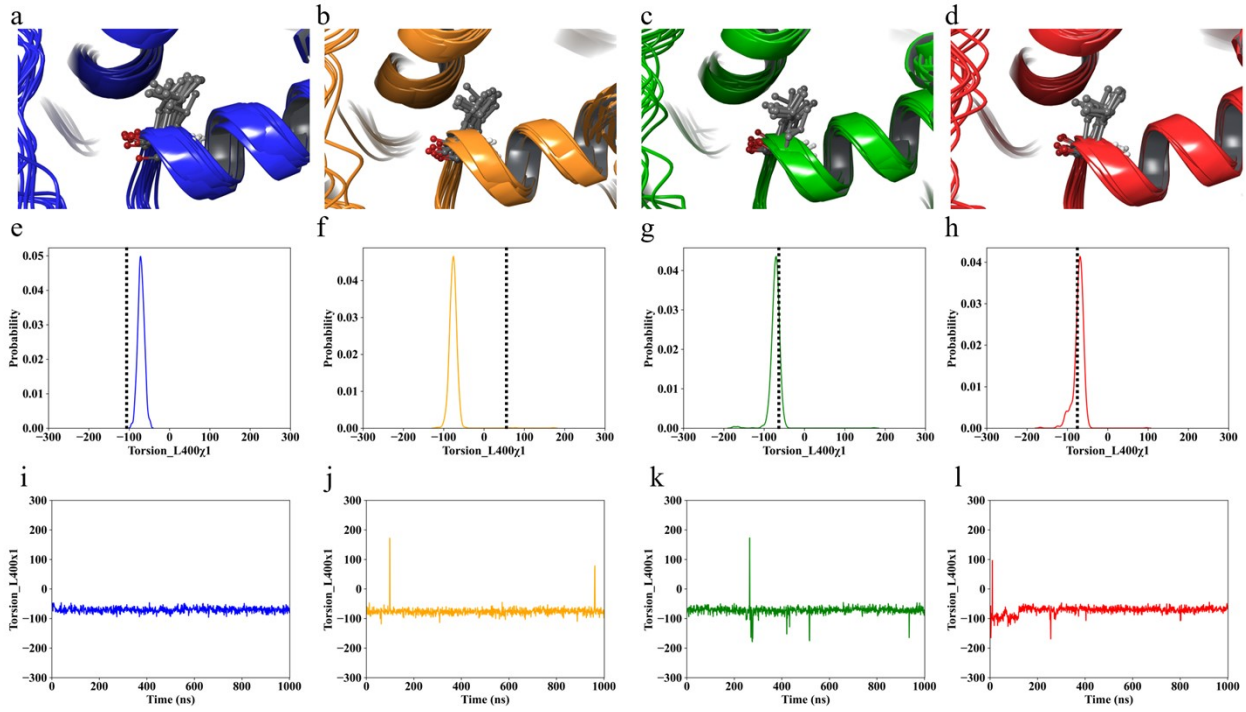


**S-Fig 8.** The torsion angle of CRY1's L400 during the MD simulation is illustrated. This is achieved by extracting 10 snapshots at intervals of every 100 ns (a-d). The KDE plot shows the distribution of CRY1's L400 χ1 (e-h) torsion angle across all simulation frames, with dashed lines denoting angles discerned in the CRY1 crystal structure. Linear graphs (i-l) present the progression of the torsion angle of L400 over time. The colors represent different structures: Apo (Blue), TH301 (Yellow), KL101 (Green), and KL201 (Red).

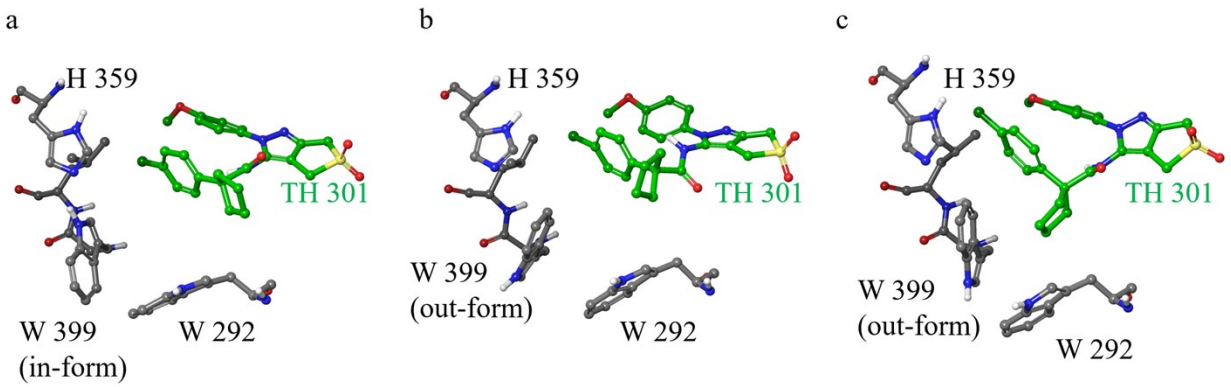


**S-Fig 9.** Extracted initial snapshots of the MD simulation of the complex between TH301 compound and mCRY1. It represents the bound forms at 0ns (a), 5ns (b), and 12ns (c) of the MD simulation.

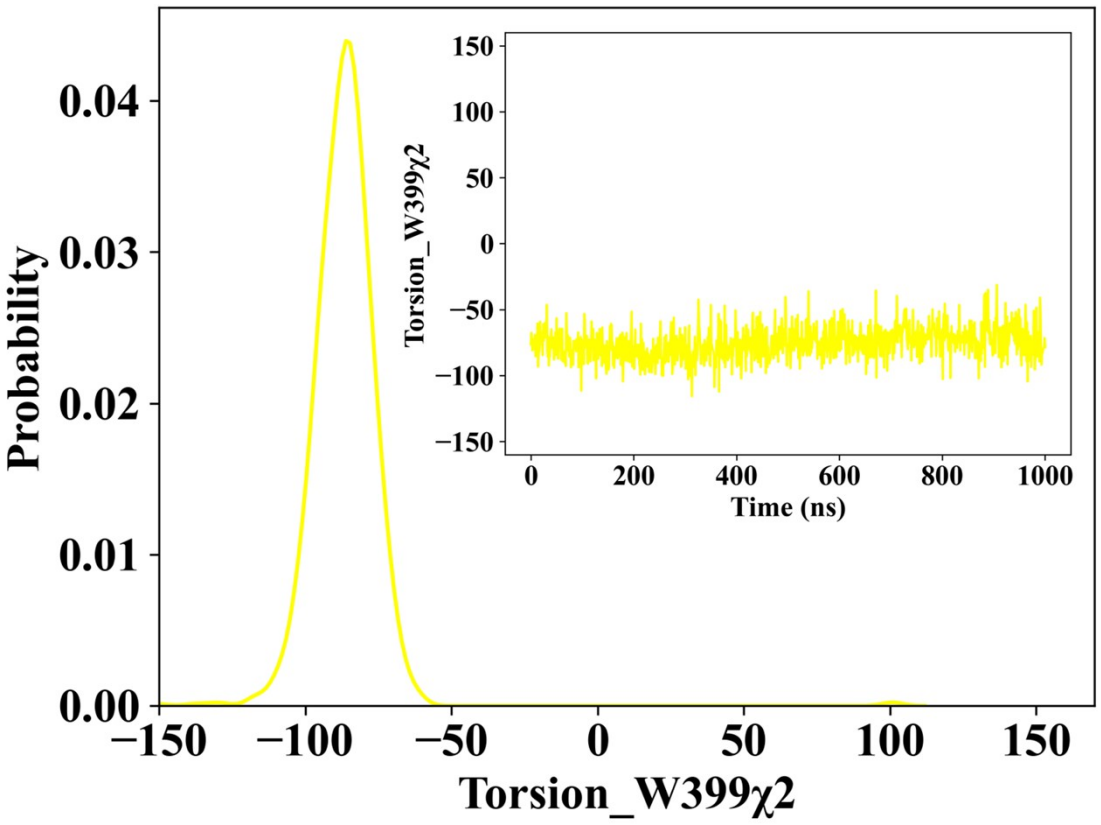


**S-Fig 10.** The MD simulation results were initialized with a manually modeled structure of W399 in the in-form conformation within the CRY1-TH301 complex. Within the MD simulation, the χ2 torsion angle of W399 is depicted by the KED plot, with the torsion angle sequentially illustrated within the graph according to the simulation time.

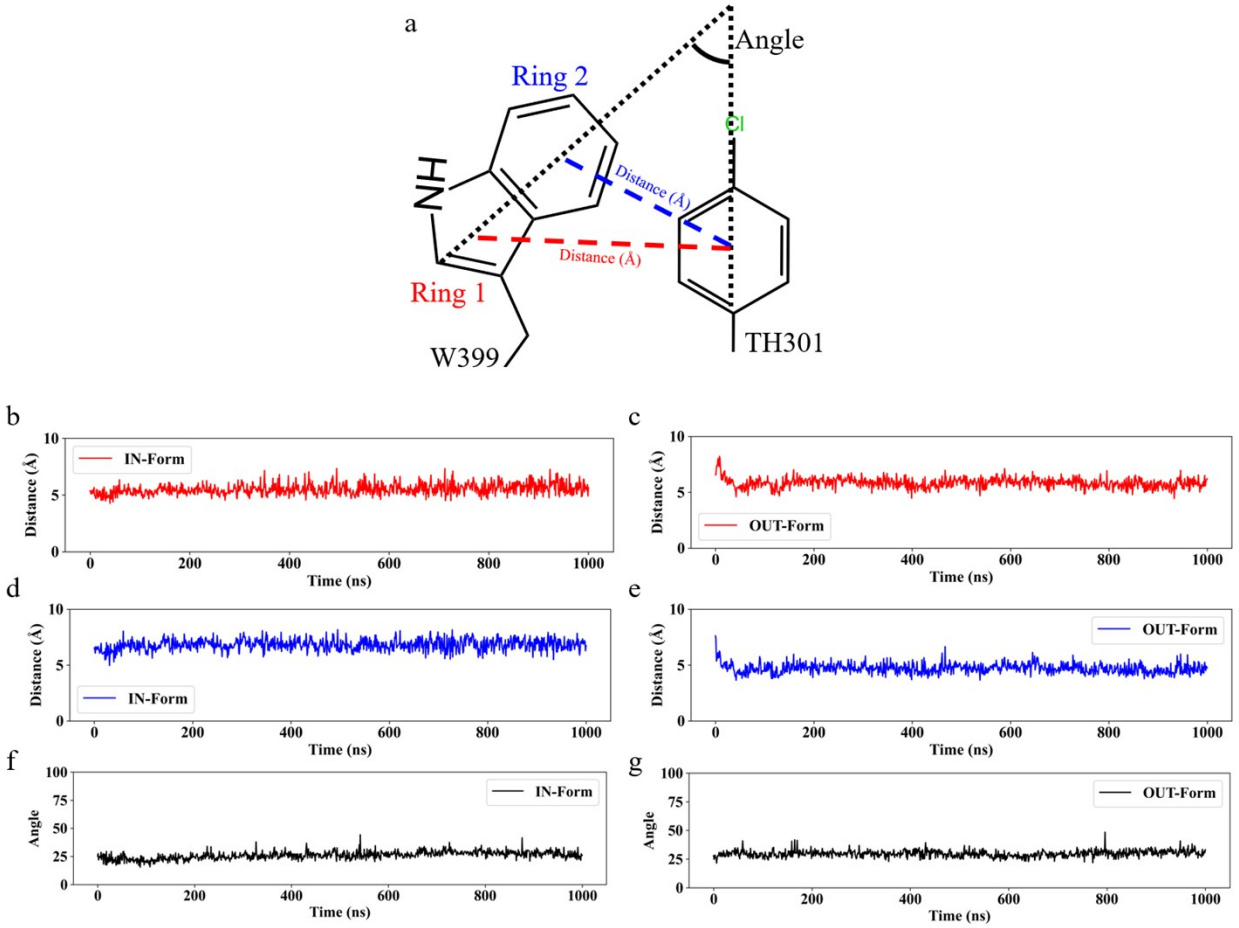


**S-Fig 11.** In standard MD simulations, the initial position of the χ2 torsion angle of W399 in the CRY-TH301 complex was set to either in-from or out-from configurations. Over a 1000 ns simulation period, the distances and angles between TH301's chlorobenzene structure and W399's two ring structures were assessed (a). (b) The distance between TH301's chlorobenzene and W399's pyrrole structure in the in-from setting, and (c) in the out-from setting. (d) The distance between TH301's chlorobenzene and W399's benzene structure in the in-from setting, and (e) in the out-from setting. (f) The angle between TH301's chlorobenzene and W399's side chain in the in-from setting, and (g) in the out-from setting.

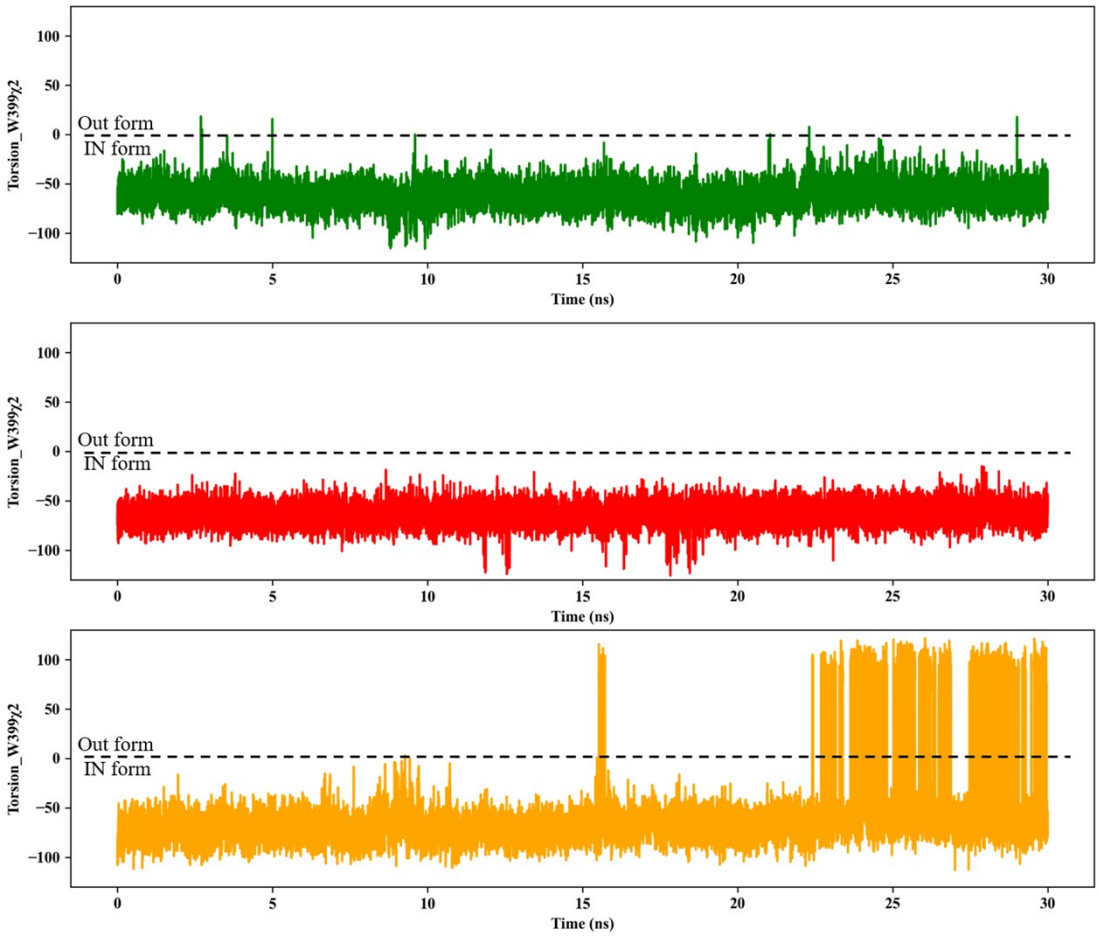


**S-Fig 12.** During the REST simulation, the χ2 torsion angle of CRY complex's W399 is depicted over time for each ligand (a-c). (a) Movement of CRY1's W399 χ2 torsion angle when bound with KL101. (b) Movement of CRY1's W399 χ2 torsion angle when bound with KL201. (c) Movement of CRY1's W399 χ2 torsion angle when bound with TH301. The colors represent different structures: KL101 (Green), KL201 (Red), and TH301 (Yellow).

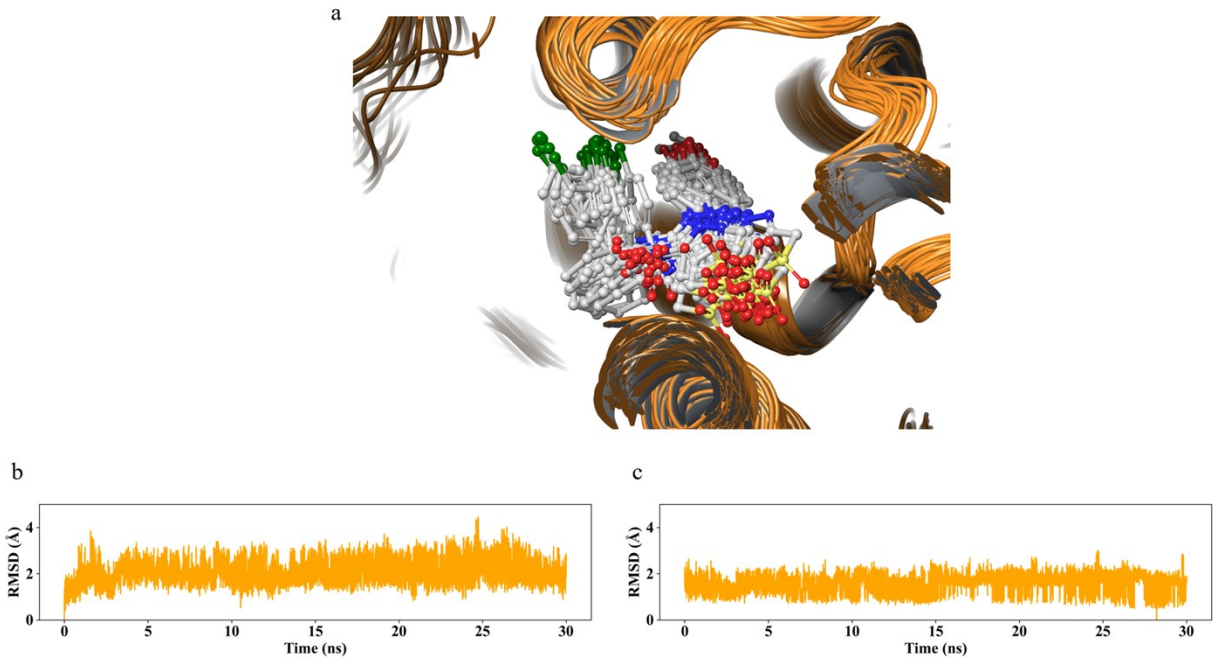


**S-Fig 13**. Observing ligand movement in CRY1 during REST Simulations. (a) Snapshots of the CRY1 and TH301 binding pose were extracted at 1 ns intervals over a 30 ns period during the REST simulation. (b) The RMSD of the ligand's movement in the Protein-Ligand Complex during the REST simulation, with the initial structure serving as the reference. (c) The RMSD of the ligand's movement in the Protein-Ligand Complex during the REST simulation, with the reference frame set to the average structure observed during the 15-30 ns period, where W399's movement was observed.

S-Table 1. Interaction energies between CRY and TH301 computed using MM-GBSA during MD simulations, and the corresponding entropy and ΔG Bind values derived from these energies.

| | ΔG Bind MM-GBSA* | Coulomb MM-GBSA* | Covalent MM-GBSA* | Hbond MM-GBSA* | Lipo MM-GBSA* | Packing MM-GBSA* | SolvGB MM-GBSA* | -TΔS | ΔG Bind |
|---|---|---|---|---|---|---|---|---|---|
| TH301 (in-form) | -84.34 | -20.62 | 1.78 | -0.94 | -29.43 | -3.10 | 33.23 | 8.56 | -10.53 |
| TH301 (out-form) | -83.06 | -17.88 | 2.11 | -0.75 | -30.83 | -4.46 | 30.90 | 8.63 | -10.46 |

* The MM-GBSA label in each column indicates it was calculated using the Schrodinger's MM-GBSA module.

S-Table 2. Exchange statistics during REST simulations of KL101, KL201, and TH301 with the mCRY1 complex. Each row represents a pair of temperature replicas, showing the number of total exchange attempts, accepted exchanges, rejected exchanges, and the resulting acceptance ratio.

| | KL101 | | | | KL201 | | | | TH301 | | | |
|---|---|---|---|---|---|---|---|---|---|---|---|---|
| Replica Pairs | Total Exchanges | No. Accepts | No. Rejects | Accept Ratio | Total Exchanges | No. Accepts | No. Rejects | Accept Ratio | Total Exchanges | No. Accepts | No. Rejects | Accept Ratio |
| T01 – T02 | 15864 | 4530 | 11334 | 0.286 | 15864 | 4501 | 11363 | 0.284 | 15864 | 4699 | 11165 | 0.296 |
| T02 – T03 | 9011 | 2659 | 6352 | 0.295 | 9011 | 2667 | 6344 | 0.296 | 9011 | 2711 | 6300 | 0.301 |
| T03 – T04 | 11326 | 3407 | 7919 | 0.301 | 11326 | 3411 | 7915 | 0.301 | 11326 | 3329 | 7997 | 0.294 |
| T04 – T05 | 10473 | 3266 | 7207 | 0.312 | 10473 | 3317 | 7156 | 0.317 | 10473 | 3191 | 7282 | 0.305 |
| T05 – T06 | 10845 | 3378 | 7467 | 0.311 | 10845 | 3326 | 7519 | 0.307 | 10845 | 3396 | 7449 | 0.313 |
| T06 – T07 | 10828 | 3382 | 7446 | 0.312 | 10828 | 3351 | 7477 | 0.309 | 10828 | 3414 | 7414 | 0.315 |
| T07 – T08 | 10679 | 3440 | 7239 | 0.322 | 10679 | 3408 | 7271 | 0.319 | 10679 | 3418 | 7261 | 0.320 |
| T08 – T09 | 10775 | 3433 | 7342 | 0.319 | 10775 | 3320 | 7455 | 0.308 | 10775 | 3451 | 7324 | 0.320 |
| T09 – T10 | 10796 | 3542 | 7254 | 0.328 | 10796 | 3443 | 7353 | 0.319 | 10796 | 3358 | 7438 | 0.311 |
| T10 – T11 | 10730 | 3513 | 7217 | 0.327 | 10730 | 3614 | 7116 | 0.337 | 10730 | 3418 | 7312 | 0.319 |
| T11 – T12 | 10746 | 3568 | 7178 | 0.332 | 10746 | 3551 | 7195 | 0.330 | 10746 | 3454 | 7292 | 0.321 |
| T12 – T13 | 10836 | 3675 | 7161 | 0.339 | 10836 | 3632 | 7204 | 0.335 | 10836 | 3489 | 7347 | 0.322 |
| T13 – T14 | 10714 | 3628 | 7086 | 0.339 | 10714 | 3618 | 7096 | 0.338 | 10714 | 3580 | 7134 | 0.334 |
| T14 – T15 | 10696 | 3623 | 7073 | 0.339 | 10696 | 3660 | 7036 | 0.342 | 10696 | 3487 | 7209 | 0.326 |
| T15 – T16 | 10821 | 3772 | 7049 | 0.349 | 10821 | 3821 | 7000 | 0.353 | 10821 | 3816 | 7005 | 0.353 |
| T16 – T17 | 10658 | 3658 | 7000 | 0.343 | 10658 | 3697 | 6961 | 0.347 | 10658 | 3753 | 6905 | 0.352 |
| T17 – T18 | 10780 | 3720 | 7060 | 0.345 | 10780 | 3872 | 6908 | 0.359 | 10780 | 3743 | 7037 | 0.347 |
| T18 – T19 | 10754 | 3829 | 6925 | 0.356 | 10754 | 3863 | 6891 | 0.359 | 10754 | 3752 | 7002 | 0.349 |
| T19 – T20 | 10848 | 3944 | 6904 | 0.364 | 10848 | 3828 | 7020 | 0.353 | 10848 | 3753 | 7095 | 0.346 |
| T20 – T21 | 10588 | 3868 | 6720 | 0.365 | 10588 | 3755 | 6833 | 0.355 | 10588 | 3655 | 6933 | 0.345 |
| T21 – T22 | 11136 | 3931 | 7205 | 0.353 | 11136 | 3816 | 7320 | 0.343 | 11136 | 3956 | 7180 | 0.355 |
| T22 – T23 | 9199 | 3255 | 5944 | 0.354 | 9199 | 3252 | 5947 | 0.354 | 9199 | 3130 | 6069 | 0.340 |
| T23 – T24 | 15676 | 5706 | 9970 | 0.364 | 15676 | 5719 | 9957 | 0.365 | 15676 | 5725 | 9951 | 0.365 |